Department of Materials Science and Engieering

A thermodynamic assessment of the BaO-MgO, BaO-CaO, $BaO-Al_2O_3$ and $BaO-SiO_2$ systems

Rui Zhang, Pekka Taskinen

Aalto University

SCIENCE + TECHNOLOGY

RESEARCH REPORT

Aalto University publication series
SCIENCE + **TECHNOLOGY** 4/2014

A thermodynamic assessment of the BaO-MgO, BaO-CaO, BaO-Al_2O_3 and BaO-SiO_2 systems

Rui Zhang, Pekka Taskinen

Aalto University
School of Chemical Technology
Department of Materials Science and Engineering
Thermodynamic and Modelling of Metallurgical Processes

Aalto University publication series
SCIENCE + **TECHNOLOGY** 4/2014

ISBN 978-952-60-5612-8
ISBN 978-952-60-5613-5 (pdf)
ISSN-L 1799-4896
ISSN 1799-4896 (printed)
ISSN 1799-490X (pdf)
http://urn.fi/URN:ISBN:978-952-60-5613-5

Unigrafia Oy
Helsinki 2014

Finland

Publication orders (printed book):
pekka.taskinen@aalto.fi,
http://materials.aalto.fi/en/research/groups/metallurgical_thermodynamics_and_modelling/

CIMO (Center of International Mobility) and Tekes (the Finnish Funding Agency for Technology and Innovation)

Aalto University

Abstract

Aalto University, P.O. Box 11000, FI-00076 Aalto www.aalto.fi

Author
Rui Zhang, Pekka Taskinen

Name of the publication
A thermodynamic assessment of the BaO-MgO, BaO-CaO, $BaO-Al_2O_3$ and $BaO-SiO_2$ systems

Publisher School of Chemical Technology

Unit Department of Materials Science and Engineering

Series Aalto University publication series SCIENCE + TECHNOLOGY 4/2014

Field of research Metallurgy

Abstract

Literature data concerning thermodynamic data for BaO including melting point, heat capacity, enthalpy increment, enthalpy of formation and entropy of formation were reviewed. The phase diagram data of the BaO-MgO, BaO-CaO, $BaO-Al_2O_3$ and $BaO-SiO_2$ systems were evaluated and taken into account in the thermodynamic assessment in the present work. Associate model was employed to describe the liquid phase in the $BaO-Al_2O_3$ and $BaO-SiO_2$ systems. Four sets of consistent thermodynamic parameters, which can explain most of the experimental data of the BaO-MgO, BaO-CaO, $BaO-Al_2O_3$ and $BaO-SiO_2$ systems, were achieved. The calculated phase diagrams of BaO-MgO, BaO-CaO, $BaO-Al_2O_3$ and $BaO-SiO_2$ systems were provided. By employing the optimized thermodynamic parameters, mixing of enthalpies of the liquid phase for the four systems and heat capacities for $BaAl_2O_4$ and $BaAl_{12}O_{19}$ were calculated and compared with the literature values.

Keywords Thermodynamic modeling; Associate model; CALPHAD; Phase diagram

ISBN (printed) 978-952-60-5612-8	**ISBN (pdf)** 978-952-60-5613-5	
ISSN-L 1799-4896	**ISSN (printed)** 1799-4896	**ISSN (pdf)** 1799-490X
Location of publisher Helsinki	**Location of printing** Helsinki	**Year** 2014
Pages 40	**urn** http://urn.fi/URN:ISBN:978-952-60-5613-5	

Table of Content

1 Introduction

Phase relations in multi-component oxide systems are generally complicated and difficult to investigate because of high temperatures for experiment. A proper multi-component oxide database should be established to improve the study of complex BaO-containing oxide systems. By thermodynamic evaluation of the MgO- CaO-Al_2O_3-SiO_2 system with additions of BaO, it's beneficial to complete the complex oxide databases, such as Mtox database used in smelting and refining [1].

In this work, the binary systems BaO-MgO, BaO-CaO, BaO-Al_2O_3 and BaO-SiO_2 were assessed using the CALPHAD (CALculation of PHAse Diagram) method. The achieved thermodynamic parameters can be served as the foundation for the future experimental research about the ternary and quaternary systems in the BaO-MgO- CaO-Al_2O_3-SiO_2 system. For the sake of simplicity, abbreviations B, A and S were used to represent BaO, Al_2O_3 and SiO_2, respectively. In the following study the abbreviations thus, $B_{10}A$, B_8A, B_7A, B_5A, B_4A, B_3A, BA, BA_6, BS, B_3S, B_2S, B_2S_3, B_5S_8, B_3S_5 and BS_2 stand for the compounds $Ba_{10}Al_2O_{13}$, $Ba_8Al_2O_{11}$, $Ba_7Al_2O_{10}$, $Ba_5Al_2O_8$, $Ba_4Al_2O_7$, $Ba_3A_2O_6$, $BaAl_2O_4$, $BaA_{l2}O_{19}$, $BaSiO_3$, Ba_3SiO_5, Ba_2SiO_4, $Ba_2Si_3O_8$, $Ba_5Si_8O_{21}$, $Ba_3Si_5O_{13}$ and $BaSi_2O_5$, respectively, if not stated otherwise.

2 Review of the experimental data

2.1 Thermodynamic data for BaO

The thermodynamic data for BaO phase including melting point, heat capacity, enthalpy increment, enthalpy of formation and entropy of formation have been measured and assessed by various authors [2-20]. In order to make the thermodynamic calculation in present work accurate and consistent, the thermodynamic properties of BaO from the database optimized by Zhou et al. [21], Zimmermann et al. [22], and SGTE substance database 1994 (SGTE94) [23] were evaluated and compared with the experimental results in the literature.

Discrepancy exists for the melting point reported by Moissan [2], Schumacher [3], Foex [4], Glushko [5], Chase et al. [6] and Seo et al. [7]. Their results are listed in Table 1. It can be seen that the value by Schumacher [3], 2196 K, is lower than those obtained in the other works [2, 4-6]. Foex [4] pointed out that the low value was probably caused by a contamination with tungsten oxide that might have been formed on the surface of the boat after the initial heating. The measured results of Foex [4] and Glushko [5] and the calculated one [7] only hold only 3-4 K differences from that of Chase et al. [6]. The melting point of 2286 K from Chase et al. [6] was accepted in this work. It represents the average temperature obtained when the data by Schumacher [3] are not considered.

Table 1. Thermodynamic data for the BaO phase per mole of the molecule.

Compound	Melting point, K	Enthalpy of formation at 298.15 K (kJ/mol)	Entropy of formation at 298.15 K (J/mol/K)

Experimental data						
BaO	2273	[2]	-548.1±2.1	[6]	72.07±0.3	[6]
	2196	[3]	-530.70	[14]	70.29±0.3	[8]
	2283	[4]	-560.82	[15]	65.90±0.1	[9]
	2290	[5]	-556.48	[16]	70.01±0.1	[10]
	2286	[6]	-552.71±0.2	[17]		
			-548.02±0.47	[18]		
			-546.16±0.54	[19]		
			-581.83±0.7	[20]		
Calculated data						
	2290	[7]	-548.06	[21]	70.29	[8]
			-553.36	[22]	69.98	[21]
			-548.10	[23]	72.07	[22]
					72.07	[23]

The heat capacity at ambient temperature was experimentally investigated by Anderson [8], Gmelin [9] and Cordfunke et al. [10]. These values extend between 55 and 300 K, 4 and 300 K, and 79 and 366 K, respectively. By smoothing and integrating the experimental data, the heat capacity of BaO up to 2200 K was derived by Irgashov et al. [11], Chekhovskoi [13] and Cordfunke et al. [10]. In the present work, the measured heat capacity from [9-13] at ambient and high temperatures were compared separately with the calculated ones from the thermodynamic functions assessed by Zhou et al. [21], Zimmermann et al. [22], and SGTE94 [23].

The comparison is shown graphically in Figures 1 and 2. A good agreement can be found at temperatures ranging from 4 K to 300 K, see Figure 1, while at high temperatures the values by Irgashov [11] and Chekhovskoi [12] show a large scatter, as shown in detail in Figure 2. At the same time, the heat capacity calculated from the assessed parameters by SGTE94 [23] fits well with Chase et al. [6], and Zhou's [21] calculation is in accordance with Cordfunke [10].

In Table 1, the entropy of formation of BaO at 298.15 K was given based on the data of Chase et al. [6], Anderson [8], Gmelin [9] and Cordfunke et al. [10]. The temperature from Gmelin [9] may be typed incorrectly as 273.15 K, instead of 298.15 K and the measurement is 5 J/mole/K lower than that from Anderson [8] and Chase et al. [6]. It was considered by Chase et al. [6] that the entropy value from Gmelin [9] should be neither at 273.15 K nor 298.15 K and must be erroneous. Chase et al. [6] calculated the entropy of formation at room temperature to be 72.069 J/mol/K by using the adopted heat capacities published in their handbook [6]. They were derived based on the measurements by Gmelin [9] with integration and correction of some typographical errors.

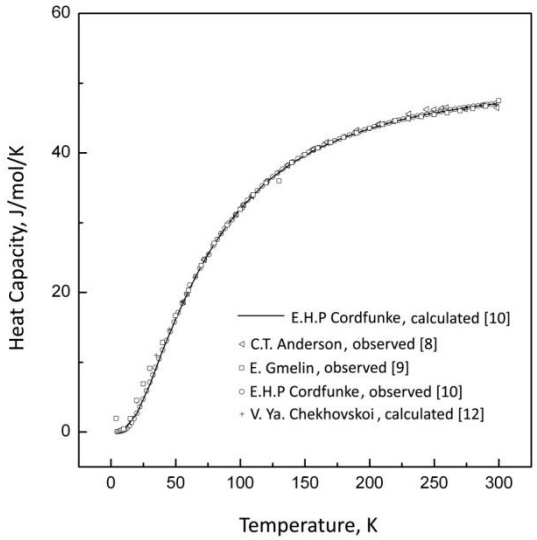

Figure 1. A comparison of heat capacity of BaO below 300 K.

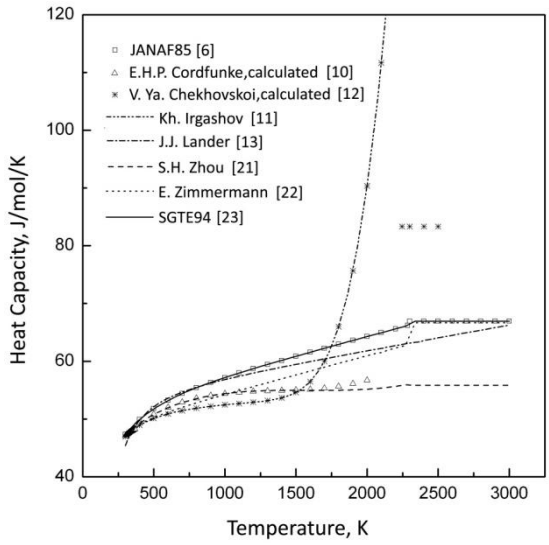

Figure 2. A comparison of heat capacity of BaO above 300 K.

Employing the drop calorimetry method, Cordfunke et al. [10], Irgashov et al. [11] and Lander [13] measured the enthalpy increment of BaO at high temperatures, and from a literature compilation, Chekhovskoi [12] calculated enthalpy increment of BaO. Their data were obtained between 390 K and 1262 K, 1171 K and 2201 K, 469 K and 876 K, and 4 K and 2500 K, respectively. Meanwhile, the authors [10-11, 13] published the polynomial equations derived from the experimental data.

In Figure 3, a comparison was made among the experimental values, polynomial equations and calculated data from the assessed parameters by Zhou et al. [21], Zimmermann et al. [22], and SGTE94 [23]. The variations of their data show minor differences except for the results from [11-12]. It can be observed that the measurement and integration by Irgashov et al. [11] and Chekhovskoi [12] show large differences at temperatures above 2000 K. The tendency resembles their [11-12] heat capacity data in Fig. 2. The calculation of SGTE94 [23] is compatible with the data by Chase et al. [6] in most temperature regions but shows small differences in respect with the

calculations by Cordfunke et al. [10], Irgashov [11] and Lander [13]. Chase et al. [6] indicated that the calorimetric data of Lander [13] was subject to bias from a calibration based on Pt and from impurities in the two samples.

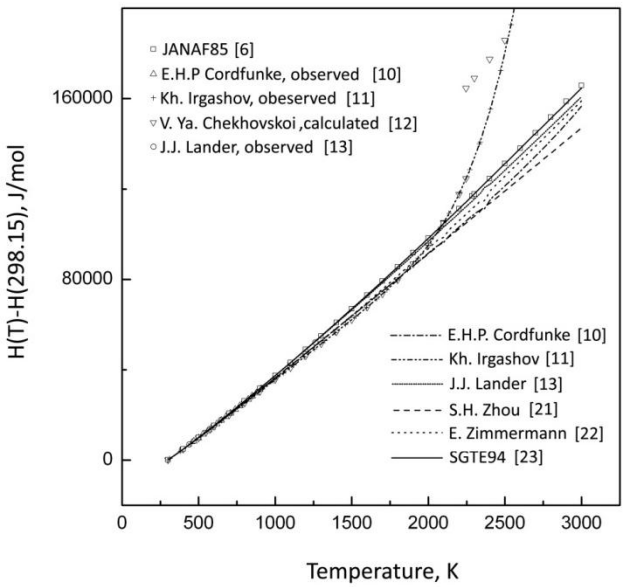

Figure 3. A comparison of enthalpy increment of BaO.

The enthalpy of formation of BaO at 298.15 K was measured by Forcrand [14], Guntz et al. [15], Zaitseva [16], Flidlider et al. [17], Fitzgibbon et al. [18] and Cordfunke et al. [19]. The values obtained are listed in Table 1.The solution calorimetry method was applied in their work to measure the enthalpy of formation, in which the molar enthalpy of solution of BaO(s) in HCl(aq) was combined with the molar enthalpy of solution of barium metal in the same solvent and with the molar enthalpy of formation of H_2O(l) to achieve the molar enthalpy of formation of BaO(s). Mah [20] employed the combustion calorimetry to investigate the enthalpy of formation for BaO. It was found that the major obstacle of combustion calorimetry was the appearance of large quantities of peroxide (BaO_2) when barium was burnt in oxygen. Therefore, solution calorimetry was preferred by most researchers

[15-19]. However, most authors did not re-measure the molar enthalpy of solution of various reactions but selected the data from previous reports, which lead to the inconsistency of molar enthalpy of BaO(s) in Table 1. The data measured by Fitzgibbon et al. [18] and Cordfunke et al. [19] and calculated by Zhou et al. [21] and SGTE94 [23] are essentially identical with each other with only a small difference. Their results are close to that adopted by Chase et al. [6] which was accepted on the basis of Fitzgibbon et al.'s [18] work.

2.2 The phase equilibrium data for BaO-MgO, BaO-CaO, $BaO-Al_2O_3$ and $BaO-SiO_2$ systems

2.2.1 BaO-MgO system

Wartenberg et al. [24] measured the liquidus and eutectic line of BaO-MgO system by a quenching technique. Van-der Kemp et al. [25] calculated phase diagram of the BaO-MgO system based on the excess thermodynamic properties, and Shukla [26] assessed this binary system using the Modified Quasichemical Model (MQM) for describing the liquid phase.

Large differences can be found in their works concerning the liquidus and the eutectic temperature. The melting point of BaO in Wartenber et al.'s [24] work is 2196 K. It is not consistent with those reported by [2-7], at the same time, although the accepted melting temperature of MgO is still under discussion [27]. The melting point of MgO reported by Wartenberg et al. [24] is very different from those reported by Mcnally et al. [28], Kanolt [29], Schneider [30]. The value 3073 K from [24] compares with 3105 ±30 K [6], 3100 ±20 K [29] and 3125 K [30]. So the misused melting points for BaO and MgO by Wartenberg et al. [24] will lead to errors for plotting the liquidus. It was reported in their work [24] that the presence of $BaCO_3$ might influence the measurement of eutectic temperature. The estimated eutectic

temperature is 1762 K and the possible value lies between 1723 K and 1773 K, based on the measurements of Wartenberg et al. [24], and the calculated value by van-der Kemp et al. [25] and Shukla [26] is 1958 K and 2092 K, respectively.

Due to the wide variation, no data were taken into account in the present work. In the literature, no phase diagram or thermodynamic data have been reported about the mutual solubility between BaO and MgO. On the basis of the published work [24-26], especially the discussion by Shukla [26], the solid solubility at both terminal solutions can be ignored.

2.2.2 BaO-CaO system

No experimental phase diagram and thermodynamic data were identified about the BaO-CaO system. Very low mutual solubilities of barium and calcium oxides in the solide state were confirmed by Flidlider et al. [31] from the calorimetric method.

Van-der Kemp et al. [25] calculated the phase diagram of this system by evaluating the excess thermodynamic functions for the binary alkaline earth oxide mixtures. Seo et al. [7] assessed the thermodynamic properties and phase diagram for the BaO-CaO system by Molecular Dynamics Simulation (MDS). Shukla [26] published the calculated phase diagram of this system by estimating the solid solubility between BaO and CaO using an equation from Blander [32]. Based on the works [25-26, 31], the mutual solubilities on both ends were estimated by taking their results as references. The calculated eutectic temperature was 2050 K [7], 2180 K [25] and 2082 K [26], respectively.

These data were not included in the present optimization because of large differences in the eutectic temperature. But the calculated liquidus by Seo et al. [7] using MDS was employed in the present calculation, due to lack of the

measured values.

2.2.3 $BaO\text{-}Al_2O_3$ system

Phase relations of the $BaO\text{-}Al_2O_3$ system have been measured by Purt et al. [33] employing thermal analysis and X-ray diffraction (XRD), in which the liquidus and solidus were published in detail. Toropov et al. [34] studied this system by equilibrium and quenching. Three stable compounds, B_3A, BA and BA_6, were reported in their papers [33-34]. Beretka et al. [35] also reported the three phases and investigated the reaction sequence of barium carbonate and aluminum oxide. They found that BA was the first to appear and then stabilize BA_6 and B_3A. Mateika et al. [36] determined the concentration range between 65-100 mol % Al_2O_3 of the $BaO\text{-}Al_2O_3$ system. In their study, the melting behavior was observed simultaneously through the chamber window using a microscope and the phase compositions were analyzed by XRD. In the reports from Mateika et al. [36], Haberey et al. [37], Kimura et al. [38] and Iyi et al. [39], the conventional 'barium hexa-aluminate' $BaAl_{12}O_{19}$ was described as two distinct phases, expressed as $BaO{\cdot}4.6Al_2O_3$ and $BaO{\cdot}6.6Al_2O_3$. Kadyrova et al. [40-41] using XRD and quenching confirmed BA_6 as the only stable phase in Al_2O_3 rich region.

In Shukla [26]'s work of the $BaO\text{-}Al_2O_3$ system, BA_6 and another compound with the chemical formula $Ba_{1.21}Al_{11}O_{17.71}$ were added in the assessment. It was mentioned that the stoichiometry of $Ba_{1.21}Al_{11}O_{17.71}$ was tentative and more experimental work was required to confirm it. In Ye et al. [42]'s assessment, only three compounds, BA, B_3A and BA_6, were included. Only BA_6 in present work was included as the stable phase in the Al_2O_3 rich region by considering the controversy of the possible existence of other phases mentioned above. In the BaO rich region, $B_{10}A$, B_8A, B_7A, B_5A and B_4A were reported to exist by [43] and [44]. Appendino [43] investigated the solid state equilibria by XRD

in the temperature range from 1173 K to 1673 K. In his study, B_4A was stable above 1231 K, under which B_5A was stable, and B_8A existed above 1323 K and B_7A was found under this temperature, and finally, $B_{10}A$ was found to be stable under 1403 K. Kovba et al. [44] studied the phase relationships by XRD and thermal analysis. According to their results [44], $B_{10}A$ and B_8A exist within larger temperature ranges as 1173 K to 1573 K compared with [43], and B_4A melts congruently at 1833 K. This melting temperature may be estimated because the temperature being studied in [44] focused between 1173 K and 1573 K. Due to the detailed description of experiments for preparing the samples and phase identification, the decomposition temperatures of $B_{10}A$, B_8A, B_7A and B_5A were calculated based on the result from Appendino [43]. The congruent melting of B_4A reported by Kovba et al. [44] was taken into account as references.

2.2.4 BaO-SiO_2 system

Eskola [45] investigated the BaO-SiO_2 binary system by quenching experiments at 1573 K to 2013 K. Four compounds B_2S, BS, B_2S_3 and BS_2 were report. The eutectic point between tridymite and B_2S was 47 wt% BaO at 1647 K. And the melting point of BS_2, according to his [45] measurement, was 1693 ±4 K. Phase region composed of two phases, B_2S_3 and BS_2, was observed. Greig [46] measured the liquidus in SiO_2-rich region by quenching and microscopic examination. He [46] pointed out that the cristobalite liquidus of was of a peculiar and its distinctive shape not hitherto encountered in silicate studies and no immiscibility should exist in this case. While based on the work by Seward et al. [47] by optical microscopy, a metastable miscibility gap was observed and even the sample containing 10 mol % BaO quenched from 1998 K was found to form the liquid immiscibility. It is favored in the study by Argyle [48] who has observed a stable liquid miscibility gap.

In the calculated phase diagram by Shukla [26], the stable liquid miscibility gap was also included. Roth and Levin [49], using quenching technique, polarizing microscope and X-ray powder diffraction, published a revised phase equilibrium diagram for the subsystem BS_2-B_2S_3. On the basis of the X-ray diffraction powder data for compounds B_3S_5, B_5S_8 and BS_2, they [49] doubted the formation of solid solution between BS_2 and B_2S_3 in Eskola's [45] work, due to the reason that instead of a continuous shift in *d* values, as expected for the solid solution, two phases of unvarying *d* values were always found for intermediate compositions. By interpretation of X-ray diffraction data of BS_2, the conclusion was made by Roth and Levin [49] that BS_2 exhibited a slowly reversible polymorphic transformation at 1623±10 K. It was confirmed by the work from Oehlschlegel [50-51]. He also reported the polymorphs of B_5S_8 and B_2S_3 that transformed at 1359 K and 1282 K respectively. Roth et al. [49] and Oehlschlegel [50-51] confirmed the existence of B_3S_5 and mentioned the unstable B_3S_5 at 1573 K transforming to well-crystallized, stable low temperature BS_2 and high temperature B_5S_8. The crystal structures of B_2S_3, B_5S_8 and BS_2 was determined and refined by Hesse [52] employing automatic Philips PW 1100 four-circle diffractometer with the program LAT by Hornastra et al. [53]. Fields et al. [54] investigated the phase equilibria in the system BaO-SrO-SiO_2 and the melting point of B_2S was found to be 2150 K. The melting point of BS observed by Jaeger et al. [55] was 1877 K and the attempts to achieve some information about a polymorphic transition of BS failed. It is reported that BS exists in two polymorphs, but the α-BS was found by Shimizu [56] to be stable at the pressure up to 120 kbar and temperatures 1113 K to 1673 K. Assignment of the X-ray diffraction pattern of α-BS to a known crystal structure was unsuccessful. Eskola [45] also tried to find out whether the barium metasilicate (BS) could be inverted into some other form by heating a sample of the crystallized compound at

1373 K overnight but no transformation took place. Consequently, the polymorphic transformation of BS at normal pressure was not considered in the present work.

Shukla [26] assessed thermodynamically the BaO-SiO_2 phase diagram. In his calculations, it was found difficult to reproduce the liquidus in high SiO_2 region as reported by Greig [46] but a miscibility gap with the upper consolute point at about 10 mol% BaO at 2026 K was estimated. The polymorphs of B_2S_3, B_5S_8 and BS_2 were not taken into account in his assessment [26].

2.3 Thermodynamic data

No thermodynamic data can be found for the BaO-MgO and BaO-CaO systems. For the BaO-Al_2O_3 system, heat capacity, enthalpy and entropy at 298.15 K for BA and BA_6 can be obtained in the handbook cited by Shabanova [57-58] and in the compilation by Barin [59]. The heat capacities for BA and BA_6 from [57-59] were employed in the present optimization. The mixing enthalpy data of these three systems are not available, maybe due to difficulties of the experiments at high temperatures. For the BaO-SiO_2 system, the calculated heat capacities of BS, B_2S, B_2S_3 and BS_2 were reported by Barin [59]. He did not identify the polymorphic properties of these phases, and therefore they were not considered in the present assessment.

3 Thermodynamic modeling

3.1 Unary phases

The Gibbs energy of component i in phase ϕ, ${}^{0}G_i^{\phi}(T) = G_i^{\phi}(T) - H_i^{SER}$, ($i$=BaO, MgO, CaO, Al_2O_3 and SiO_2) was expressed by equation:

$${}^{0}G_i^{\phi}(T) = a + bT + cT\ln T + dT^{2} + eT^{-1} + fT^{3} + gT^{7} + hT^{-9} \quad (1)$$

H_i^{SER} is the sum of the enthalpies of the elements at 298.15 K and 1 bar in their stable states (Stable Element Reference, denoted as SER); T is the absolute temperature. In this work, the Gibbs energy functions for pure BaO are consistent with SGTE94 according to the evaluation in Section 2.1. The Gibbs energy expression for pure MgO was taken from Hallstedt [60], and the Gibbs energy functions for pure CaO and Al_2O_3 were retained from a previous assessment by Hallstedt [61], and that of pure SiO_2 was adopted from Barry [62].

3.2 Solution phases

Liquid, BaO-based, MgO-based, CaO-based, Al_2O_3-based and SiO_2-based solid solutions exist in the BaO-MgO, BaO-CaO, BaO-Al_2O_3 and BaO-SiO_2 systems respectively. Their Gibbs energy functions were described by the following expression:

$$G_m^{\phi} - H^{SER} = x_{BaO}\,{}^{0}G_{BaO}^{\phi} + x_i\,{}^{0}G_i^{\phi} + RT(x_{BaO}\ln x_{BaO} + x_i \ln x_i) + {}^{E}G_m \quad (2)$$

where x_{BaO} and x_i are the mol fractions of BaO and component i (i=MgO, CaO, Al_2O_3 and SiO_2), ${}^{E}G_m$ is the excess Gibbs energy, which was described

by the Redlich-Kister polynomials [63] as:

$$^{E}G_m = x_{BaO}x_i\,{}^{l}L_{BaO\bullet i} = x_{BaO}x_i[{}^{0}L+{}^{1}L(x_{BaO}-x_i)] \quad (3)$$

where ^{l}L is the interaction parameter between BaO and component i (i=MgO, CaO, Al_2O_3 and SiO_2) to be optimized in the present work. The general temperature dependent form of the interaction parameter $^{l}L = a + bT$ was used.

In the BaO-Al_2O_3 system, both associate and substitutional solution models were employed to describe the liquid phase. In the BaO-SiO_2 system, associate model was used for the description of liquid phase. The Gibbs energy function for substitutional solution model is the same as equations (2) and (3). For associate model in both BaO-Al_2O_3 and BaO-SiO_2 systems, it was assumed to be constituted of three species: BaO, Al_2O_3 (or SiO_2) and $BaAl_2O_4$ (or $BaSiO_3$). The molar Gibbs energy of liquid can be expressed as follows:

$$\begin{aligned} G_m^{\phi} - H^{SER} = {} & y_{BaO}\,{}^{0}G_{BaO}^{Liq} + y_{Al_2O_3(SiO_2)}\,{}^{0}G_{Al_2O_3(SiO_2)}^{Liq} \\ & + y_{BaAl_2O_4(BaSiO_3)}\,{}^{0}G_{BaAl_2O_4(BaSiO_3)}^{Liq} \\ & + RT(y_{BaO}\ln y_{BaO} + y_{Al_2O_3(SiO_2)}\ln y_{Al_2O_3(SiO_2)} \\ & + RT(y_{BaAl_2O_4(BaSiO_3)}\ln y_{BaAl_2O_4(BaSiO_3)}) + {}^{E}G_m \end{aligned} \quad (4)$$

where y represents the mole fractions of BaO, Al_2O_3 (or SiO_2) and $BaAl_2O_4$ (or $BaSiO_3$) in the liquid, and $^{E}G_m$ can be described as:

$$\begin{aligned} {}^{E}G_m = {} & y_{BaO}y_p\,{}^{n}L_{BaO\bullet p} + y_{BaO}y_q\,{}^{n}L_{BaO\bullet q} + y_p y_q\,{}^{n}L_{p\bullet q} \\ & + y_{BaO}y_p[{}^{0}L_{BaO\bullet p}+{}^{1}L_{BaO\bullet p}(y_{BaO}-y_p)] \\ & + y_{BaO}y_q[{}^{0}L_{BaO\bullet q}+{}^{1}L_{BaO\bullet q}(y_{BaO}-y_q)] \\ & + y_p y_q[{}^{0}L_{p\bullet q}+{}^{1}L_{p\bullet q}(y_p-y_q)] \end{aligned} \quad (5)$$

where p is Al_2O_3 or SiO_2, and q is $BaAl_2O_4$ or $BaSiO_3$ respectively. ${}^nL$ is the interaction parameter among three species in liquid, which will be assessed in present work. The general form of ${}^nL$ is the same as ${}^lL$.

It should be noted that according to the evaluation of previous literature data in Section 2.2, the terminal solid solutions (BaO-based, MgO-based, Al_2O_3-based and SiO_2-based solutions) in the BaO-MgO, BaO-Al_2O_3 and BaO-SiO_2 systems were taken as pure oxides. The mutual solid solubilities of BaO and CaO in halite in the BaO-CaO system were considered in the present work. Substitutional solution model, (BaO, CaO), was applied to describe the solution phases in the solid BaO-CaO system.

3.3 Compounds

No compounds were reported to exist in the BaO-MgO and BaO-CaO systems. In the BaO-Al_2O_3 and BaO-SiO_2 systems, $B_{10}A$, B_8A, B_7A, B_5A, B_4A, B_3A, BA, BA_6, BS, B_3S, B_2S, B_2S_3, B_5S_8, B_3S_5 and BS_2 were confirmed. There are heat capacity data for BA and BA_6. The molar Gibbs energy functions of them were evaluated as:

$$ {}^0G_{BA} - H_{Ba}^{SER} - 2H_{Al}^{SER} - 4H_O^{SER} = A_1 + B_1T + C_1T\ln T + D_1T^2 + E_1T^{-1} \quad (6) $$

$$ {}^0G_{BA_6} - H_{Ba}^{SER} - 12H_{Al}^{SER} - 19H_O^{SER} = A_2 + B_2T + C_2T\ln T + D_2T^2 + E_2T^{-1} \quad (7) $$

where H_i^{SER} is the enthalpy of element i in its stable form at 298.15 K and 1 bar, and SER stands for Stable Element Reference. Due to lack of thermochemical data, the Gibbs energy expressions for the other stoichiometric compounds mentioned above were described by the

Neumann-Kopp rule. Their Gibbs energy functions were given by:

$$^{0}G_{B_nA_m} = n^{0}G^{S}_{BaO} + m^{0}G^{S}_{Al_2O_3} + A_i + B_iT \quad (8)$$

$$^{0}G_{B_nS_m} = n^{0}G^{S}_{BaO} + m^{0}G^{S}_{SiO_2} + C_i + D_iT \quad (9)$$

where A_i, B_i, C_i and D_i are the enthalpy and entropy of formation of the compounds from the pure oxides. The parameters A_i and B_i were optimized in the present work.

4 Results and discussion

After critical evaluation in Section 2.1, the thermodynamic data of pure BaO phase from SGTE94 were selected in the present work. The thermodynamic optimization was performed using PARROT module of the Thermo-calc software package [64]. Step-by-step optimization procedure was adopted and the experimental data from the literature sources [33, 34, 43-46, 49-55] were employed. Each piece of information was given a certain weight indicating the experimental uncertainty. The weights were adjusted and optimization was repeated until reaching a satisfactory description of most experimental results. The parameters already obtained were slightly adjusted using all the selected experimental data simultaneously to achieve the best overall fit.

The optimized thermodynamic parameters obtained have been listed in Table 2. The calculated phase diagrams compared with the literature values [7, 24-26, 33-36, 49-55] are shown in Figs. 4-8. The measured and calculated invariant equilibria are compared in Table 3. It can be observed from figures and tables that a good agreement can be achieved in most regions, while some contradictions exist, which will be discussed below.

Table 2. Summary of thermodynamic parameters describing the BaO-MgO, BaO-CaO, BaO-Al_2O_3 and BaO-SiO_2 systems.*

BaO-MgO

Liquid: ${}^0L$ = -11000+7*T, ${}^1L$ = -1.3*T

BaO-CaO

Liquid: ${}^0L$ = -12011+6*T, ${}^1L$ = 2*T

BaO-Al_2O_3 [a]

Liquid: ${}^0L_{BaO,Al_2O_3}$ = -175716.6-26*T ${}^0L_{BaAl_2O_4,Al_2O_3}$ = -340120-40*T

${}^0L_{BaO,BaAl_2O_4}$ = -340101-40*T ${}^0L_{BaAl_2O_4}$ = -139122.3+50*T

BA: -2596313.52+362.036*T-74.16*T*Ln(T)-0.00885775*T^2+731345.7*$T^{(-1)}$

BA_6: -11140656.33-300.03*T-105.4*T*Ln(T)-0.005048*T^2+1581988*$T^{(-1)}$

B_3A: 3* G^S_{BaO} + $G^S_{Al_2O_3}$ -447035+73.5* T

$B_{10}A$: 10* G^S_{BaO} + $G^S_{Al_2O_3}$ -576815+140*T

B_7A : 7* G^S_{BaO} + $G^S_{Al_2O_3}$ -539871+126.5*T

B_5A: 5* G^S_{BaO} + $G^S_{Al_2O_3}$ -510418+114.6*T

B_8A: 8* G^S_{BaO} + $G^S_{Al_2O_3}$ -377588-2*T

B_4A: 4* G^S_{BaO} + $G^S_{Al_2O_3}$ -425269+50*T

$BaO\text{-}Al_2O_3$ [b]

Liquid: ${}^0L_{BaO,Al_2O_3}$ = -383247+19.8*T ${}^1L_{BaO,Al_2O_3}$ = -98605+10.06*T

${}^2L_{BaO,Al_2O_3}$ = -80622*T

BA: -2452496.97+307.433*T-74.1*T*Ln(T)-0.00885918*T^2+731503.1*$T^{(-1)}$

BA_6: -11128809.8-300.87*T-105.4*T*Ln(T)-0.0050476*T^2+1582462.4*$T^{(-1)}$

B_3A: 3* G^S_{BaO} + $G^S_{Al_2O_3}$ -364830+70.86* T

$B_{10}A$: 10* G^S_{BaO} + $G^S_{Al_2O_3}$ -576815+140*T

B_7A : 7* G^S_{BaO} + $G^S_{Al_2O_3}$ -436228+115.57*T

B_5A: 5* G^S_{BaO} + $G^S_{Al_2O_3}$ -409400+100.77*T

B_8A: 8* G^S_{BaO} + $G^S_{Al_2O_3}$ -354288+50.3*T

B_4A: 4* G^S_{BaO} + $G^S_{Al_2O_3}$ -358918+62.44*T

BaO-SiO_2

Liquid: ${}^0L_{BaO,SiO_2}$ =-204789+9.9*T ${}^0L_{BaSiO_3,SiO_2}$ =-38534.7+25*T

${}^0L_{BaO,BaSiO_3}$ =-569630.39+10*T ${}^0L_{BaSiO_3}$ =-257197.59+24.6*T

BS : G^S_{BaO} + $G^S_{SiO_2}$ -229651.02+15.1* T

B_3S : 3* G^S_{BaO} + $G^S_{SiO_2}$ -320174.3+32* T

B_2S : 2* G^S_{BaO} + $G^S_{SiO_2}$ --293949.6+24* T

H-B_2S_3 : 2* G^S_{BaO} +3* $G^S_{SiO_2}$ -474588.20+29* T

L-B_2S_3 : 2* G^S_{BaO} +3* $G^S_{SiO_2}$ -478065.4+31.7* T

H-B_5S_8 : 5* G^S_{BaO} +8* $G^S_{SiO_2}$ -1192822.5+72.7* T

L-B_5S_8 : 5* G^S_{BaO} +8* $G^S_{SiO_2}$ -1197200.1+75.9* T

B_3S_5 : 3* G^S_{BaO} +5* $G^S_{SiO_2}$ -713503.11+41.21* T

H-BS_2 : G^S_{BaO} +2* $G^S_{SiO_2}$ -234403.5+10* T

L-BS_2 : G^S_{BaO} +2* $G^S_{SiO_2}$ -240886.05+14* T

* All values are given in SI units (J, mol, K), [a] means the calculated data using associate model, [b] means the calculated data using substitutional model.

Table 3. Invariant equilibria in the BaO-MgO, BaO-CaO, BaO-Al_2O_3 and BaO-SiO_2 systems*

Equilibrium	T, K	Composition	Reference
BaO-MgO		mol. % MgO	
Liquid+BaO+MgO	1762	0.44	[22]
	1958	0.22	[23]
	2092	0.24	[24]
	2092	0.24	Present work [a]

BaO-CaO		mol. % CaO	
Liquid+BaO+CaO	2180	0.14	[23]
	2050	0.2	[8]
	2082	0.28	[24]
	2149	0.26	Present work [a]
$BaO-Al_2O_3$		mol. % Al_2O_3	
Liquid+B_3A	2023	0.25	[32]
	1893	0.25	[31]
	1877	0.25	[24]
	1893	0.25	Present work [a]
	1893	0.25	Present work [b]
Liquid+BA	2103	0.5	[32]
	2088	0.5	[31]
	2561	0.5	[24]
	2088	0.5	Present work [a]
	2088	0.5	Present work [b]
Liquid+BA_6	2173	0.857	[32]
	2188	0.857	[31]
	2188	0.857	Present work [a]
	2188	0.857	Present work [b]
Liquid+B_4A	1833	0.2	[42]
	1845	0.2	[24]
	1884	0.2	Present work [a]
	1889	0.2	Present work [b]
Liquid+B_3A+BA	1983	0.304	[32]
	1753	0.304	[31]
	1866	0.271	[24]
	1891	0.266	Present work [a]
	1891	0.268	Present work [b]
Liquid+BA+BA_6	2063	0.648	[32]
	1893	0.770	[31]
	2095	0.282	[24]
	2023	0.637	Present work [a]
	2001	0.637	Present work [b]
Liquid+BA_6+Al_2O_3	2163	0.880	[32]
	2148	0.880	[31]
	2138	0.736	[24]
	2176	0.903	Present work [a]

	2165	0.917	Present work [b]
Liquid+BaO+B_8A	1885	0.119	[24]
	1992	0.103	Present work [a]
	1932	0.131	Present work [b]
Liquid+B_8A+B_4A	1829	0.172	[24]
	1874	0.178	Present work [a]
	1885	0.179	Present work [b]
Liquid+B_4A+B_3A	1880	0.220	Present work [a]
	1891	0.218	Present work [b]
$B_{10}A$+BAO+B_8A	Below 1403	0.091	[41]
	1403	0.091	Present work [a]
	1401	0.091	Present work [b]
B_8A+$B_{10}A$+B_4A	Above 1323	0.111	[41]
	1328	0.111	Present work [a]
	1329	0.111	Present work [b]
B_7A+$B_{10}A$+B_4A	Below 1323	0.125	[41]
	1232	0.125	[24]
	1232	0.125	Present work [a]
	1229	0.125	Present work [b]
B_4A+B_7A+B_3A	Above 1213	0.2	[41]
	1213	0.2	[24]
	1216	0.2	Present work [a]
	1212	0.2	Present work [b]
B_5A+B_7A+B_3A	Below 1213	0.167	[41]
	1173	0.167	[24]
	1175	0.167	Present work [a]
	1174	0.167	Present work [b]
BaO-SiO_2		mol. % SiO_2	
Liquid+H-BS_2	1693	0.667	[45]
	1693	0.667	[49]
	1695	0.667	Present work [a]
Liquid+ H-B_5S_8	1719	0.615	[49]
	1718	0.615	Present work [a]
Liquid+ H-B_2S_3	1720	0.6	[49]
	1720	0.6	Present work [a]
Liquid+BS	1877	0.5	[55]
	1877	0.5	Present work [a]
Liquid+ B_2S	2150	0.333	[54]

	2150	0.333	Present work [a]
	>2023	0.333	[55]
Liquid+B_3S	2125	0.26	Present work [a]
H-BS_2+ L-BS_2	1623	0.667	[49]
	1623	0.667	[50]
	1623	0.667	Present work [a]
H-B_5S_8 +L-B_5S_8	1358	0.615	[50]
	1358	0.615	Present work [a]
H-B_2S_3	1282	0.6	[50]
	1283	0.6	Present work [a]
B_3S_5+H-B_5S_8+L-BS_2	1573	0.625	[50]
	1573	0.625	Present work [a]
Liquid +B_2S+BS	1824	0.47	[45]
	1768	0.468	Present work [a]
Liquid+BS+ H-B_2S_3	1708	0.572	[45]
	1704	0.571	Present work [a]
Liquid+ H-B_5S_8+B_3S_5	1696	0.654	[49]
	1696	0.659	[50]
	1703	0.652	Present work [a]
Liquid+H-BS_2+B_3S_5	1683	0.66	[49]
	1695	0.665	Present work [a]
Liquid+L-BS_2+Tridymite	1645	0.75	[45]
	1642	0.74	[46]
	1340	0.859	Present work [a]

[a] means the calculated data using associate model, [b] means the calculated data using substitutional model.

For the BaO-MgO system, the assessed data in this work fits well with Shukla's calculation [26] but not with the measurements from [24]. As mentioned in section 2.2, the reported melting points of MgO and BaO [24] are much lower than those given in the other sources [2-7, 29-30]. Waternberg [24] et al. measured only four points to construct phase diagram of the BaO-MgO system. Their data [24] were not taken into account in the present calculations or in [24]. Van-der Kemp et al. [25] reported that the estimated excess parameters for the BaO-MgO system showed the largest

deviation from ideal mixing behavior. In this case, the present calculations and [26] are in reasonable agreement. Future work, for example a DTA/DSC study, should be done to measure the eutectic temperature.

For the BaO-CaO system, the calculated eutectic temperature, 2149 K, is not consistent with that in work [7, 25-26]. They also scatter greatly from each other: 2059 K in [7], 2180 K in [25] and 2082 K in [26]. In the absence of experimental data, the mutual solubilities of BaO and CaO in halite were estimated taking [25-26] as references. The estimated solubility ranges agree well with [25-26].

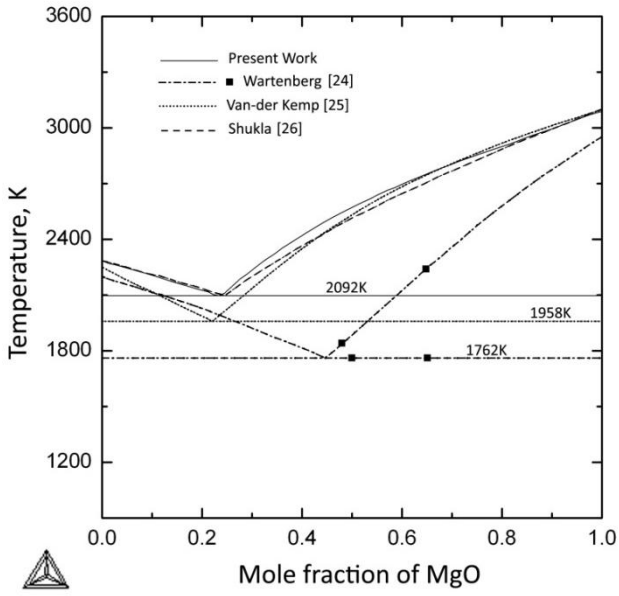

Figure 4. Calculated phase diagram of BaO-MgO system, compared with references [24-26].

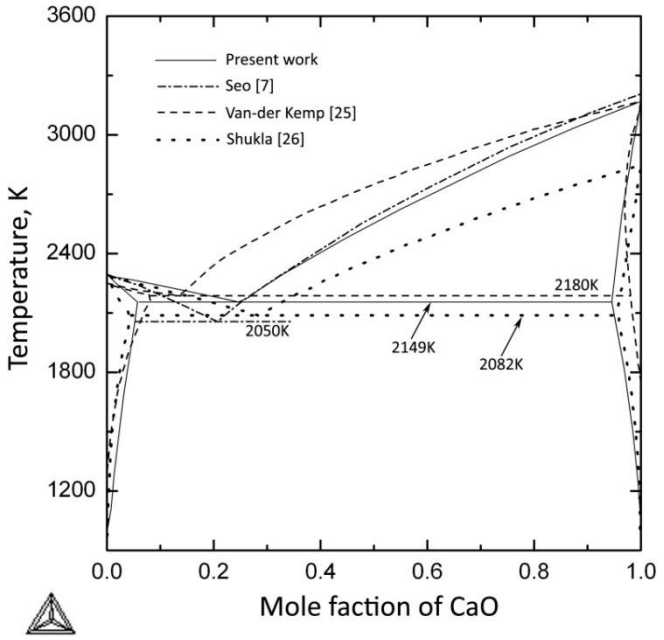

Figure 5. Calculated phase diagram of BaO-CaO system, compared with references [7, 25-26].

For the BaO-Al_2O_3 system, the difficulty in measuring the liquidus and the melting points at high temperatures leads to large uncertainty of experimental results. The measurements by Purt et al. [33] and Toropov et al. [34] showed great discrepancies on the liquidus, ranging from 20 mol % to 100 mol % Al_2O_3, and as to the melting point for B_3A. Detailed experimental procedures have been published in their papers [33-34], and so both the results were given certain weights during optimization.

It was found that the calculated liquidus using both the associate and substitutional solution models are consistent with [34] in most part of the phase diagram. The calculated invariant reactions cannot reproduce well both experimental sets. They are relatively close to the data from [34]. In the published phase diagrams [33-34] in the BaO-rich region, the confirmed compounds $B_{10}A$, B_8A, B_7A, B_5A and B_4A [43-44] were omitted, which leads to differences when the liquidus line was based on measured points [33-34].

Shukla [26] assessed the $BaO\text{-}Al_2O_3$ system by considering the existence of these five compounds. His calculation for the melting point of BA shows a huge deviation from the experimental data. In present work, the decomposition temperatures of compounds, $B_{10}A$, B_8A, B_7A, B_5A, and B_4A, were assessed based on the results by Appendino [43]. Much experimental work is still required to establish accurately the temperatures of decomposition for these binary compounds.

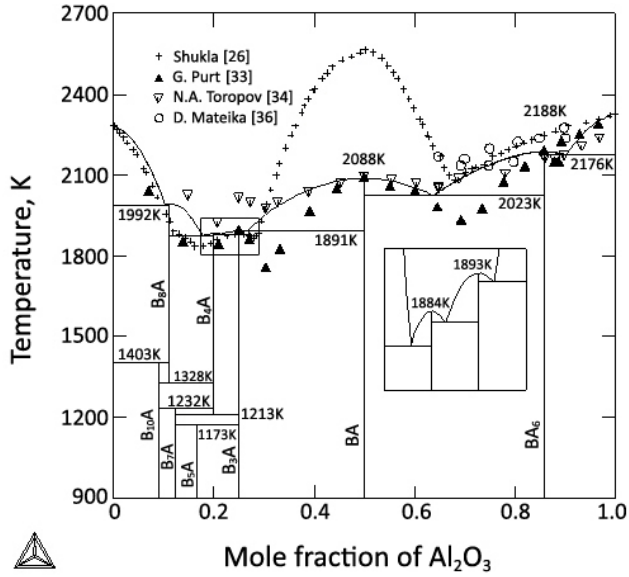

Figure 6. Calculated phase diagram of $BaO\text{-}Al_2O_3$ system using associate model, compared with references [26, 33-34, 36].

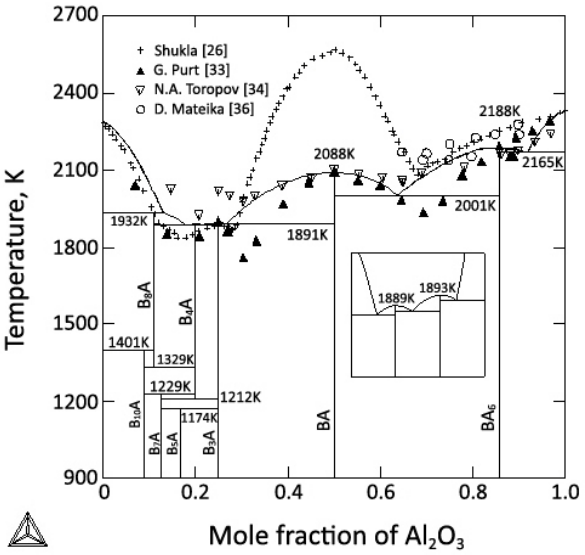

Figure 7. Calculated phase diagram of BaO-Al_2O_3 system using substitutional model, compared with references [26, 33-34, 36].

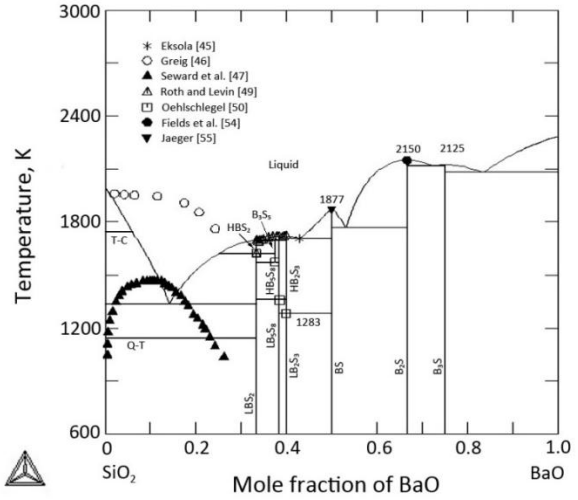

Figure 8. Calculated phase diagram of BaO-SiO_2 system using associate model, compared with references [26, 45-55].

For the BaO-SiO_2 system, three silica polymorphs, quarts, tridymite and cristobalite, were adopted in the present assessment. Large discrepancy can be found at SiO_2-rich part for the liquidus. Based on Seward's [47] measurement, a metastable miscibility gap existed below liquidus, while

Greig [46] reported the liquidus with a strange shape and with no phase separation. The present calculated liquidus is situated between Seward and Greig's [46] work. Detailed experiments are required to confirm the liquidus of SiO_2-rich part. The polymorphic transformation of BS, B_2S_3, B_5S_8 and BS_2 were taken into account in the present work and the calculated results agree well with the experimental work by Roth and Levin [49].

The enthalpies of mixing at various temperatures of the BaO-MgO, BaO-CaO, BaO-Al_2O_3 and BaO-SiO_2 systems (all referred to pure liquid oxides) have been calculated in Figs. 9-13. Due to lack of experimental measurements, the predictions in the present work were only compared with the calculated

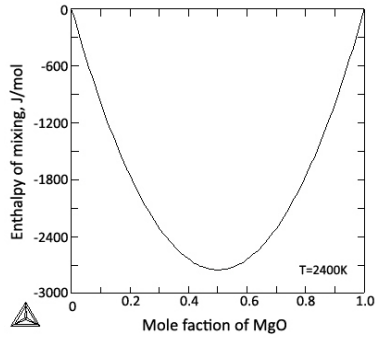

Figure 9. Calculated enthalpy of mixing for BaO-MgO liquid at 2400 K (referred to liquid BaO and liquid MgO).

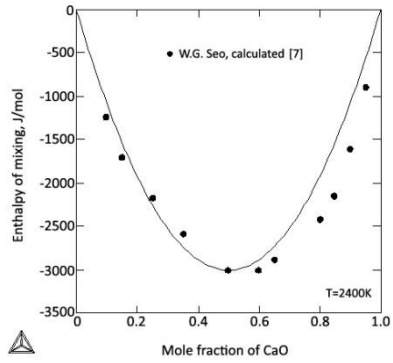

Figure 10. Calculated enthalpy of mixing for BaO-CaO liquid at 2400 K, compared with calculated value [7] (referred to liquid BaO and liquid CaO).

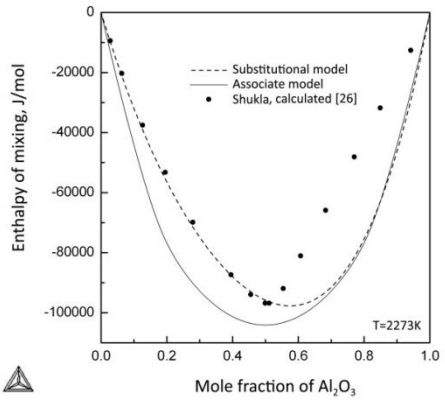

Figure 11. Calculated enthalpy of mixing for $BaO\text{-}Al_2O_3$ liquid at 2273 K using associate model and substitutional model, compared with calculated value [26] (referred to liquid BaO and liquid Al_2O_3).

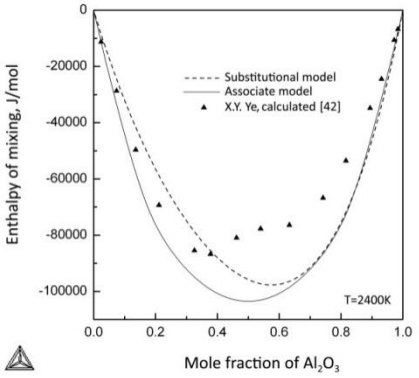

Figure 12. Calculated enthalpy of mixing for $BaO\text{-}Al_2O_3$ liquid at 2400 K using associate model and substitutional model, compared with calculated value [42] (referred to liquid BaO and liquid Al_2O_3).

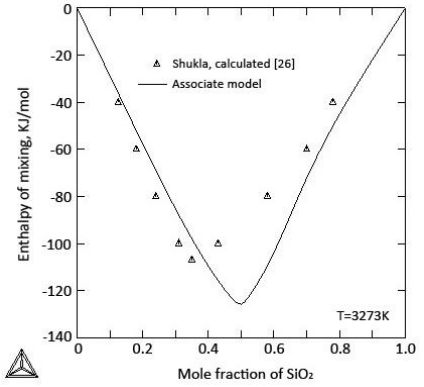

Figure 13. Calculated enthalpy of mixing for $BaO\text{-}SiO_2$ liquid at 3273 K, compared with calculated value [26] (referred to liquid BaO and liquid SiO_2).

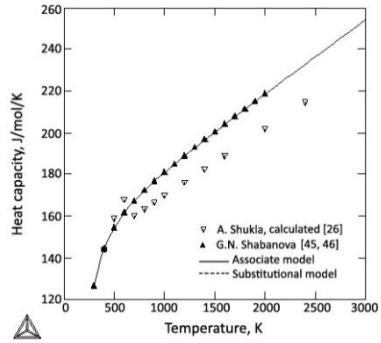

Figure 14. Calculated heat capacity for $BaAl_2O_4$, compared with data from the literature [26, 45-46].

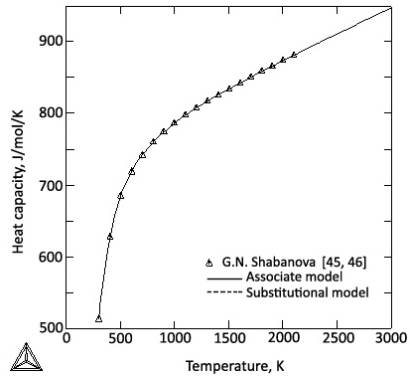

Figure 15. Calculated heat capacity of $BaAl_2O_{19}$, compared with references [45-46].

values from [7, 26, 42]. The comparison shows a reasonable agreement. In this work, in the BaO-Al_2O_3 assessment employing the associate model, BA was selected as an associate. A valley showing minimum value can be observed in Fig. 11 and 12 at composition of the BA (50 mol % Al_2O_3) which shows strong interactions of molecules in the liquid oxide at the composition around that of BA phase (characterized by the close interaction parameters of ${}^0L_{BaO,BaAl_2O_4}$ and ${}^0L_{BaAl_2O_4,Al_2O_3}$ in Table 2).

When using associate model to calculate the enthalpy of mixing for the liquid

oxide, it generates a deeper valley showing minimum point compared with the substitutional solution model, as shown in Fig. 11 and 12, and the minimum values of the curve are shifted from 57.6 mol % to 50 mol % Al_2O_3 and 58.1 mol % to 50 mol % Al_2O_3 respectively. X.Y. Ye et al. [42] employed a two-sublattice model for the ionic oxide solutions and Shukla [26] modeled the liquid phase by MQM, with $BaAl_2$ added as an associate. Both the associate and substitutional solution models were applied in this work to present liquid phase. The same tendency in Fig. 10 for present and Shukla's [26] works can be observed that the minimum points of the curves focus around 50 mol % Al_2O_3 because of the associates included in the models for liquid phase. The differences in Fig. 11 may result from the models adopted by the different authors to describe the liquid phase.

For the BaO-SiO_2 system, BS was selected as an associate in modeling the liquid phase. It can be observed from Fig. 13 that calculation employing associate model presents the minimum point around 50 mol % SiO_2 where the associate exists. The difference between Shukla's [26] work and the present calculation may be caused by the different models used to describe the liquid phase. The comparisons between the calculated heat capacity of BA and BA_6 in the present work and the experimental results from [43-44] were plotted in Figs. 14-15. The assessed values reproduce the previous data by [43-44] well.

5 Conclusions

Thermodynamic data of BaO was critically evaluated and compared with the available experimental values from the literature [2-20]. The stability functions for pure BaO from SGTE94 [23] were accepted and employed in the present work for the thermodynamic optimization. Phase diagrams for the BaO-MgO, BaO-CaO, BaO- Al_2O_3 and BaO-SiO_2 systems were calculated thermodynamically and compared with the literature data [24-26, 33-34, 36]. For the BaO-CaO system, the liquidus data assessed from Seo et al. [8] by MDS were included in the present assessment due to the absence of experimental measurements.

Associate and substitutional solution models were applied to describe the liquid oxide phase in the BaO-Al_2O_3 assessment. The assessed phase diagrams using both the models were compared and no large difference were found to exist between them. The calculated heat capacities of $BaAl_2O_4$ (BA) and $BaAl_{12}O_{19}$ (BA_6) were compared with the data from [26, 45-46]. A good agreement was observed. Associate model was employed for the description of liquid phase of the BaO-SiO_2 system. Discrepancies can be found at SiO_2-rich part that experimental works [45-48] show different results about whether miscibility gap should exist or not. New experimental data are needed to confirm the phase relations. The enthalpies of mixing of the liquid oxide for the four systems were calculated, using the thermodynamic model parameters obtained in the present work. A comparison was performed with the calculated data from [7, 26, 42] due to lack of experimental measurements.

6 Acknowledgements

The authors are grateful to CIMO and Tekes for the financial support. Great thanks are to be expressed to Professor Guven Akdogan of Stellenbosch University (Stellenbosch, South Africa) for the valuable guidance and discussion.

7 References

[1] MTOX, Release Notes for Version 7.0 of Mtox Database, National Physical Laboratory, Teddington, UK, 2011.

[2] H. Moissan, Compt. Rend., 134 (1902) 136-142.

[3] E.E. Schumacher, J. Am. Ceram. Soc., 48 (1926) 396-405.

[4] M. Foex, Solar Energy, 9 (1965) 61-67.

[5] V.P. Glushko (Ed.), Nauka, Moscow (1981) 379-387.

[6] M.W. Chase (Ed.), JANAF Thermochemical Tables, 3rd edition, J. Phys. Chem. Ref. Data, 14 (1985) 348-350.

[7] W.P. Seo, D.H. Zhou, F. Tsukihashi, Mater. Trans., 46 (2005) 643-650.

[8] C.T. Anderson, J. Am. Ceram. Soc., 57 (1935) 429-431.

[9] E. Gmelin, Z. Naturforsch., 24 (1969) 1794-1800.

[10] E.H.P Cordfunke, R.R. van-der Laan, J.C. van Miltenburg, J. Phys. Chem. Solids, 55 (1994) 77-84.

[11] K. Irgashov, V.D. Tarasov, Teplofizika Vysokikh Temp., 21 (1983) 688-691.

[12] V.Y. Chekhovskoi, V.D. Tarasov, Zh. Fiz. Khim., 64 (1990) 2-16.

[13] J.J. Lander, J. Am. Ceram. Soc., 73 (1951) 5794-5797.

[14] D. Forcrand, R. Ann. Chim. Phys., 15 (1908) 458.

[15] M.A. Guntz, F. Benoit, Bull. Soc. Chim., 35 (1924) 709-728.

[16] L.S. Zaitseva, Izvest. Akad. Nauk. SSSR Ser. Fiz., 20 (1956) 1123-1126.

[17] G.V. Flidlider, P.V. Kovtunenko, A.A. Bundel, Russ. J. Phys. Chem., 40 (1966) 1168-1172.

[18] G.C. Fitzgibbon, E.J. Huber, C.E. Holley, J. Chem. Thermodynam., 5 (1973) 577-582.

[19] E.H.P Cordfunke, R.J.M. Konings, W. Ouweltjes, J. Chem. Thermodynam., 22 (1990) 991-996.

[20] A.D. Mah, U. S. Bur. Mines Rep. Invest. No.6171 (1963).

[21] S.H. Zhou, R. Arroyave, C.A. Randall, Z.K. Liu, J. Am. Ceram. Soc., 88 (2005) 1943-1948.

[22] E. Zimmermann, K. Hack, D. Neuschutz, Calphad, 19 (1995) 119-127.

[23] The SGTE Substance Database, Version 1994, SGTE (Scientific Group Thermodata Europe), Grenoble, France (1994).

[24] H.V. Wartenberg, E. Prophet, Z. Anorg. Allgem. Chem., 208 (1932) 369-379.

[25] W.J.M. van-der Kemp, J.G. Blok, P.R. van-der Linde, H.A.J. Oonk, A. Schuijff, Calphad, 18 (1994) 255-267.

[26] A. Shukla, Ph.D. thesis, Ecole Polytechnique de Montreal, Canada (2012).

[27] C. Ronchi, M. Sheindlin, J. Appl. Phys., 90 (2001) 3325-3331.

[28] R.N. Macnally, F.I. Peters, P.H. Ribbe, J. Am. Ceram. Soc., 44 (1961) 491.

[29] C.W. Knaolt, Bull. Bur. Stand., 10 (1914) 295.

[30] S.J. Schneider, U. S. Nat. Bur. Stand. Monograph (1963) 68.

[31] G.V. Flidlider, T.V. Kovtunenko, E.V. Kiseleva, A.A. Bundel, Russ, J. Phys. Chem., 40 (1966) 1329-1331.

[32] M. Blander, Thermodynamic Properties of Molten Salt Solutions, in 'Selected Topics in the Physical Chemistry of Molten Salts', edited by M. Blander (Interscience Publishers, Inc., New York) (1962).

[33] G. Purt, Radex-Rundschau, 4 (1960) 198-202.

[34] N.A. Toropov, F.Y. Galakhov, Dokl. Akad. Nauk SSSR, 82 (1952) 69-70.

[35] J. Beretka, T. Brown, Aust. J. Chem., 26 (1973) 2527-2531.

[36] D. Mateika, H. Laudan, J. Cryst. Growth, 46 (1979) 85-90.

[37] F. Haberey, G. Oehlschlegel, K. Sahl, Ber. Dt. Keram. Ges., 54 (1977) 373-378.

[38] S. Kimura, E. Bannai, I. Shindo, Mat. Res. Bull., 17 (1982) 209-215.

[39] N. Iyi, S. Takekawa, Y. Bando, S. Kimura, J. Solid State Chem., 47 (1983) 34-40.

[40] Z.R. Kadyrova, N.A. Syrazhiddinov, S.K. Tuganova, Dokl. Akad. Nauk Resp. Uzb., 4 (1996) 26-27.

[41] Z.R. Kadyrova, D.A. Daminova, Uzb. Khim. Zh., 4 (1997) 8-12.

[42] X.Y. Ye, W.D. Zhuang, C.Y. Deng, W.X.Yuan, Z.Y. Qiao, Calphad, 30 (2006) 349-353.

[43] P. Appendino, Ann. Chim., 61 (1971) 822-830.

[44] L.M. Kovba, L.N. Lykova, E.V. Antipov, M.V. Paromova, O.N. Rozanova, Russ. J. Inorg. Chem., 32 (1987) 301-302.

[45] P. Eskola, Am. J. Sci., 5th Ser., 4 (1922) 331-375.

[46] J.W. Greig, Am. J. Sci., 5th Ser., 13 (1927) 1-44.

[47] T.P. Seward, D.R. Uhlmann, D. Turnbull, J. Am. Ceram. Soc., 51 (1968) 278-285.

[48] J.F. Argyle, F.A. Hummel, Phys. Chem. Glasses, 46 (1963) 103-105.

[49] R.S. Roth, E.M. Levin, J. Res. Nat. Bur. Stand, 62 (1959) 193-200.

[50] G. Von Oehlschlegel, Glastechn. Ber., 44 (1971) 194-204.

[51] G. Von Oehlschlegel, W. Ohnmacht, Glastechn. Ber., 48 (1975) 232-236.

[52] K.F. Hesse, F. Liebau, Z. Kristallogr., 153 (1980) 3-17.

[53] J. Hornstra, H. Vossers, Philips Technische Rundschau, 33 (1973/74) 65-78.

[54] J.M.J. Fields, P.S. Dear, J.J.J Brown, J. Am. Ceram. Soc., 55 (1972) 585-588.

[55] F.M. Jaeger, H.S. Van Klooster, Proc. K. Ned. Akad. Wet., 18 (1916) 896-913.

[56] Y. Shimizu, Y. Syono, S. Akimoto, High Temp.-High Press., 2 (1970) 113-120.

[57] G.N. Shabanova, Refractories and Industrial Ceram., 44 (2003) 254-259.

[58] G.N. Shabanova, Refractories and Industrial Ceram., 45 (2004) 25-30.

[59] I. Barin, Thermochemical Data of Pure Substances, 3rd edition, VCH Verlagsgesellschaft mbH, Weinheim (Germany) & VCH Publishers, Inc., New York, USA, (1995) 148-150.

[60] B. Hallstedt, J. Am. Ceram. Soc., 75 (1992) 1497-1507.

[61] B. Hallstedt, J. Am. Ceram. Soc., 73 (1990) 15-23.

[62] T.I. Barry, 'CaO-SiO_2 Assessment' reported by J.R. Taylor and A.T. Dinsdale, CALPHAD, Amsterdam, the Netherlands, 1990 (Unpublished Work).

[63] O. Redlich, A. Kister, Industrial and Engineering Chemistry, 40 (1948) 345-348.

[64] B. Sundman, B. Jansson, J.-O. Andersson, Calphad, 9 (1985) 153-190.

Phase relations in multi-component oxide systems are generally complicated and difficult to investigate because of high temperatures for experiment. A proper multi-component oxide database should be established to improve the study of complex BaO-containing oxide systems. By thermodynamic evaluation of the MgO-CaO-Al_2O_3-SiO_2 system with additions of BaO, it's beneficial to complete the complex oxide databases, such as Mtox database used in smelting and refining.

Aalto-ST 4/2014

ISBN 978-952-60-5612-8
ISBN 978-952-60-5613-5 (pdf)
ISSN-L 1799-4896
ISSN 1799-4896
ISSN 1799-490X (pdf)

Aalto University
School of Chemical Technology
Department of Materials Science and Engieering
www.aalto.fi